Molecular Cell, Vol. 7, 907–913, April, 2001, Copyright ©2001 by Cell Press

Three-Dimensional Structure of the Anaphase-Promoting Complex

Christian Gieffers,*‖ Prakash Dube,†‖ J. Robin Harris,‡ Holger Stark,† and Jan-Michael Peters*§
*Research Institute of Molecular Pathology (IMP)
Dr. Bohr-Gasse 7
A-1030 Vienna
Austria
†Max Planck Institute for Biophysical Chemistry
Department of Cellular Biochemistry
Am Fassberg 11
D-37077 Goettingen
Germany
‡University of Mainz
Institute of Zoology
D-55099 Mainz
Germany

Summary

The anaphase-promoting complex (APC) is a cell cycle–regulated ubiquitin-protein ligase, composed of at least 11 subunits, that controls progression through mitosis and G1. Using cryo-electron microscopy and angular reconstitution, we have obtained a three-dimensional model of the human APC at a resolution of 24 Å. The APC has a complex asymmetric structure 140 Å × 140 Å × 135 Å in size, in which an outer protein wall surrounds a large inner cavity. We discuss the possibility that this cavity represents a reaction chamber in which ubiquitination reactions take place, analogous to the inner cavities formed by other protein machines such as the 26S proteasome and chaperone complexes. This cage hypothesis could help to explain the great subunit complexity of the APC.

Introduction

The anaphase-promoting complex/cyclosome (APC) is a ubiquitin-protein ligase that controls important transitions in mitosis by ubiquitinating regulatory proteins and thereby targeting them for proteolysis by the 26S proteasome (Irniger et al., 1995; King et al., 1995; Sudakin et al., 1995). To initiate sister chromatid separation, the APC has to ubiquitinate the anaphase inhibitor securin, whereas exit from mitosis requires the ubiquitination of B-type cyclins (reviewed by Morgan, 1999; Peters, 1999; Nasmyth et al., 2000). These reactions depend on the activator proteins CDC20 and CDH1 that transiently associate with the APC at the end of mitosis and in G1/G0, respectively (reviewed by Morgan, 1999; Zachariae and Nasmyth, 1999). In ubiquitination reactions, the APC fulfills the role of a ubiquitin-protein ligase (E3); i.e., it allows the transfer of ubiquitin residues from ubiquitin-conjugating (E2) enzymes to specific substrate proteins. This reaction results in the formation of multiubiquitin chains, which are thought to function as a recognition signal for the 26S proteasome (reviewed by Peters 1994; Varshavsky, 1997; Baumeister et al., 1998).

Based on sequence homologies and biochemical properties, two types of ubiquitin-protein ligases can presently be distinguished. HECT domain proteins (proteins with *h*omology to the *E*6-AP *C t*erminus) form covalent ubiquitin thioesters before they transfer the ubiquitin residue to the substrate protein (Scheffner et al., 1995). All other known ubiquitin-protein ligases are characterized by the presence of a RING finger, a protein domain that is stabilized by the coordination of two atoms of zinc. RING fingers are not known to form ubiquitin thioester intermediates but have been shown to directly bind to ubiquitin-conjugating enzymes (Zheng et al., 2000). RING fingers are found in otherwise diverse ubiquitin-protein ligases, such as the APC, SCF and VHL complexes, c-CBL, MDM2, and Ubr1p, proteins that have been implicated in regulating a large variety of different cellular processes (reviewed by Joazeiro and Weissman, 2000). In SCF and VHL complexes, the RING finger subunit binds to cullin proteins (reviewed by Deshaies, 1999; Tyers and Willems, 1999) that are distantly related to the APC subunit APC2 (Yu et al., 1998; Zachariae et al., 1998). The crystal structures of several subunits of SCF and VHL complexes and of fragments of MDM2, c-CBL, and of the HECT protein E6-AP have been solved (Kussie et al., 1996, Huang et al., 1999; Stebbins et al., 1999, Schulman et al., 2000; Zheng et al., 2000). The molecular mechanism by which these proteins mediate substrate ubiquitination is not understood, but the cocrystal structure of c-CBL bound to a substrate peptide and an E2 enzyme suggests that RING finger ubiquitin-protein ligases may serve as scaffolds that position substrates and E2 enzymes optimally for ubiquitin transfer (Zheng et al., 2000).

Even less is known about the structure and the mechanism of the APC. The APC is unusual among ubiquitin-protein ligases with respect to its subunit complexity. Eleven core subunits have been identified in the human APC (Yu et al., 1998; Grossberger et al., 1999; Gmachl et al., 2000), not including regulatory molecules such as CDC20, CDH1, and MAD2. In contrast, other ubiquitin-protein ligases are only known to be composed of one or a few subunits; for example, five subunits have been identified in SCF and VHL complexes (reviewed by Deshaies, 1999; Tyers and Willems, 1999). The RING finger domain of the APC is contained in its smallest known subunit, the 10 kDa protein APC11 (Zachariae et al., 1998, Gmachl et al., 2000). Remarkably, this protein alone is sufficient to mediate ubiquitination reactions in the presence of UBC4 and the ubiquitin-activating enzyme E1 (Gmachl et al., 2000; Leverson et al., 2000). In contrast to holo-APC, the activity of APC11 cannot be stimulated by CDH1, and APC11 shows a reduced substrate specificity compared to holo-APC (Gmachl et al., 2000). These observations imply that APC11 may mediate ubiquitination reactions within the holo-APC, whereas the function of some of the other APC subunits

§To whom correspondence should be addressed (e-mail: peters@nt.imp.univie.ac.at).
‖These authors contributed equally to this work.

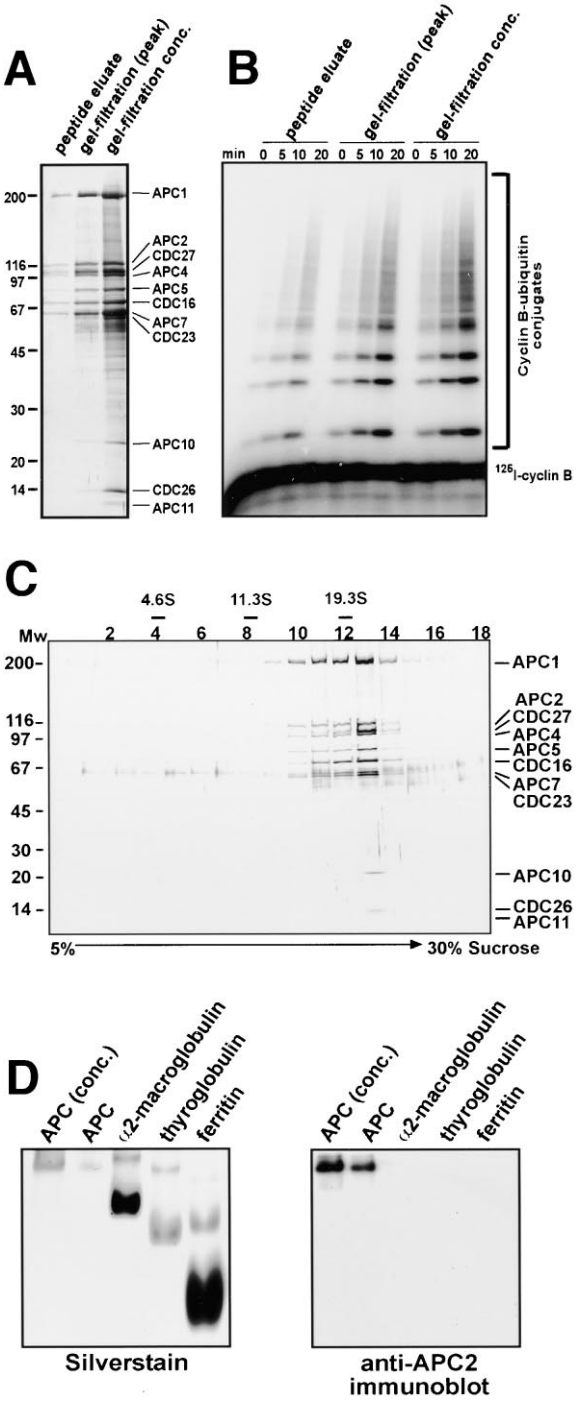

Figure 1. Purification and Characterization of Human APC

(A) Silver stain analysis of purified APC. Fractions of isolated APC taken from different steps of the purification procedure, as indicated, were separated by SDS–PAGE, and proteins were subsequently detected by silver staining. The positions of APC subunits and marker proteins are indicated.

(B) Analysis of enzymatic activity. APC from the fractions shown in (A) were tested for their ubiquitin-protein ligase activity in an in vitro ubiquitination assay using [^{125}I]cyclin B as a substrate. Samples taken at the indicated time points were analyzed by SDS–PAGE and phosphorimaging. (Input levels for the peptide eluate and the gel filtration peak fraction were 5 μl and 2.5 μl for the concentrated gel-filtration fraction).

(C) Sucrose density gradient centrifugation. Purified human APC was separated on a 5%–30% sucrose density gradient and analyzed by SDS–PAGE and silver staining. The positions of the APC subunits and the fraction numbers are indicated. At the top, the migration of marker proteins of known S values are shown (bovine serum albumin, 4.6S; catalase, 11.3S; and thyroglobulin, 19.3S).

(D) Native electrophoreses: APC samples corresponding to the fractions' peptide eluate and gel-filtration peak (see Figure 1A) and marker proteins were electrophoresed on a 5% native polyacrylamide gel at 60V for 10 hr, and proteins were visualized by silver staining (left panel). APC was identified by immunoblotting on a parallel gel using an APC2 antibody (right panel).

may be to regulate the activity of APC11 and to modulate its substrate specificity.

Understanding the mechanism of the APC and the function of all of its subunits will not be possible without solving its structure. Because the APC is a nonabundant complex whose reconstitution from recombinant subunits has not been achieved yet, crystallizing the whole APC is presently not feasible. We have, therefore, developed a method that allows the isolation of small amounts of highly purified native human APC. By analysis of these samples by cryo-electron microscopy, we derived a three-dimensional (3D) model of the APC with a resolution of 24 Å. This model reveals that the APC has a complex asymmetric structure in which an outer protein wall surrounds a large inner cavity or cage. We discuss the possibility that this cavity represents a reaction chamber in which cell cycle–regulated ubiquitination reactions take place, analogous to the inner cavities formed by other protein machines such as the 26S proteasome and chaperone complexes.

Results

Isolation and Characterization of Native Human APC

APC was immunoprecipitated from extracts of logarithmically growing HeLa cells using CDC27 peptide antibodies. Bound complexes were subsequently eluted in their native form with an excess of antigenic peptide. The peptide was subsequently separated from the eluted protein by gel filtration chromatography (data not shown). SDS–PAGE and silver staining analysis of the resulting fractions revealed all known 11 subunits of human APC, whose identity was confirmed by immunoblotting (Figure 1A and data not shown). In the presence of purified ubiquitin, E1 and E2 enzymes, and ATP, the APC fractions were able to ubiquitinate a radiolabeled fragment of cyclin B in a dose-dependent manner (Figure 1B), suggesting that the employed method allows the preparation of active APC in a highly purified soluble form.

To assess the physical homogeneity of the APC in the purified fractions, we separated peptide eluates by density gradient centrifugation, analytical gel filtration, and native gel electrophoresis. SDS–PAGE and silver staining revealed that all APC subunits cosedimented during sucrose density gradient centrifugation (Figure 1C). Calibration of the gradient with marker proteins suggested that the majority of APC (fraction 13) sedi-

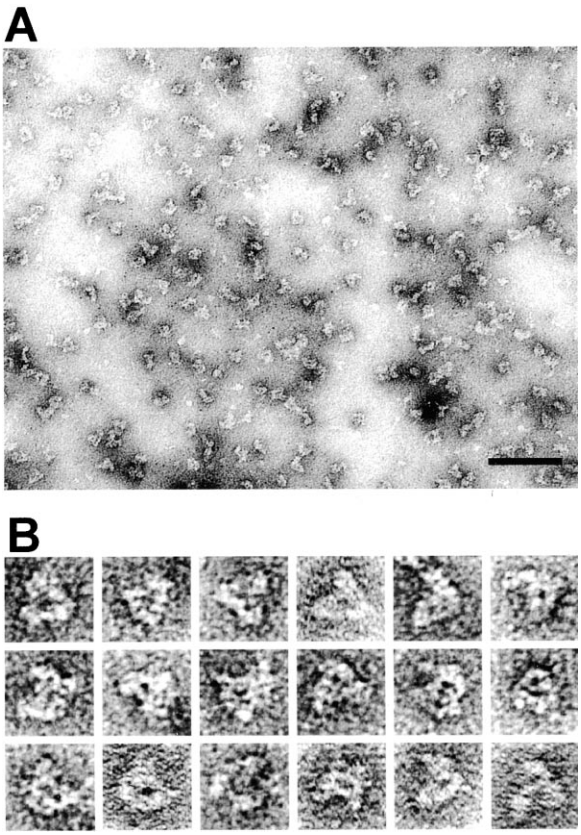

Figure 2. Electron Microscopic Analysis of APC Negatively Stained with 2% Ammonium Molybdate

(A) Low magnification micrograph (the scale bar is 75 nm).
(B) Gallery of selected APC particles representing different views of the APC.

ments with a sedimentation coefficient of 22–23S. For a globular protein complex, this S value would correspond to a molecular mass of 815,000–870,000. Separation of purified APC fractions on a TSG-G5000PW×l column indicated a molecular mass of 870,000 (data not shown). Although the precise stoichiometry of APC subunits is not yet known, our data are consistent with the possibility that each subunit is present once per complex. In native gels, APC migrated as one predominant band that could be detected by silver staining and immunoblotting with monoclonal APC2 antibodies (Figure 1D). When concentrated APC samples were analyzed, a much less abundant, more slowly migrating second band could also be detected, possibly representing a dimeric form of the APC. However, such forms do not seem to form stably in solution, because no evidence for dimeric APC was obtained in density gradient centrifugation experiments (Figure 1C). Together, our results suggest that purified APC fractions predominantly contain APC particles of 22–23S.

Electron Microscopy of Negatively Stained APC

To obtain insight into the structure of the APC, we analyzed purified APC fractions by negative staining and transmission electron microscopy. Staining with ammonium molybdate revealed distinct particles with a diameter of approximately 15 nm (Figure 2A). Although most particles were of similar size, their shape was heterogeneous. Some particles had a triangular or V-shaped appearance, but many particles had a more irregular shape (Figure 2B). Some negative stain could be detected in the center of most particles, suggesting that heavy metal ions accumulated in a central cavity or groove of the complexes. The heterogeneity of particle images suggested that the APC is able to adsorb to the grid surface in many different orientations, resulting in different image projections that represent different views of the APC.

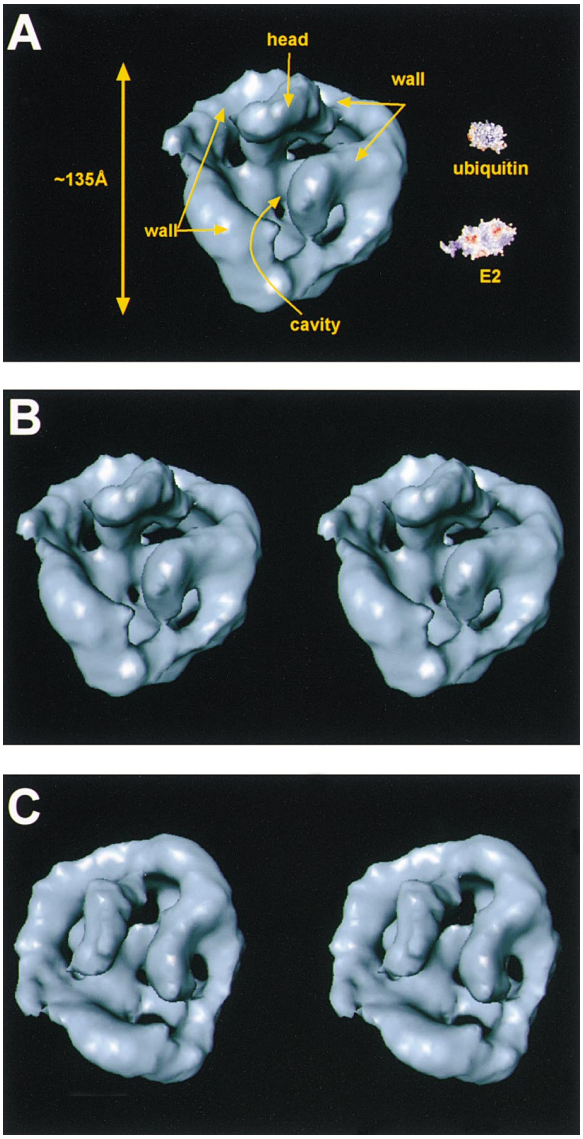

Figure 3. 3D Model of the APC Obtained by Cryo-Electron Microscopy

(A) Front view of the APC at 24 Å resolution. The size of the complex and the most prominent structural features (wall, head, and cavity) are indicated. The sizes of ubiquitin (Vijay-Kumar et al., 1987) and E2-C (Jiang and Basavappa, 1999) are shown in comparison to the APC
(B) Stereo front view of HeLa cell APC.
(C) Stereo top view of the APC.

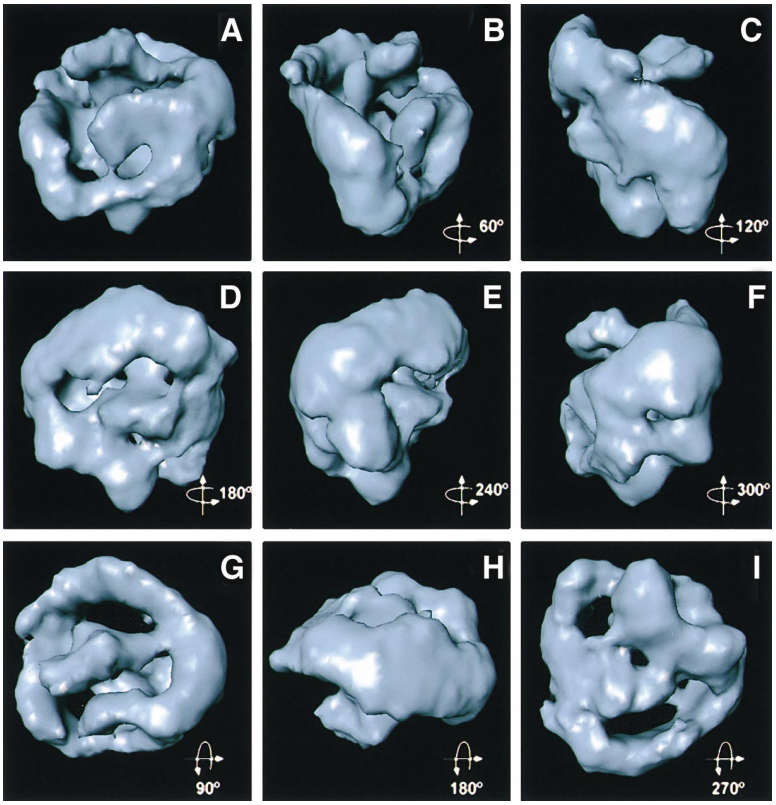

Figure 4. Gallery of the APC at 24 Å resolution

Shown is a front view of the APC (A) that is either tilted stepwise along the vertical axis by 60° ([A]–[F]) or along the horizontal axis by 90° ([G]–[I]), as indicated.

3D Structure of the APC Obtained by Cryo-Electron Microscopy

To obtain detailed insight into the native structure of the APC, we performed cryo-electron microscopy. Purified APC samples were imaged using liquid nitrogen–temperature electron microscopy. About 13,000 molecular images of randomly orientated APC particles were interactively collected from digitized micrographs. A first set of characteristic APC views was obtained by multivariate statistical analysis and automatic classification. After angular reconstitution, a preliminary low-resolution 3D structure was derived. Subsequently, the resolution of the structure was reiteratively improved by generating a large number of reference images and performing multiple cycles of multireference alignment, automatic classification, and angular reconstitution. Using this procedure, a 3D model of the APC with a final resolution of 24 Å was generated. For the surface representation, a molecular volume of 999,205 A^3, which represents an APC mass of 844,000, was used to select the threshold values.

A stereo view of the 3D model of human APC is shown in Figure 3B. We refer to this view as the front view and describe the relative position of individual parts of the structure with respect to this orientation. Figure 3C shows a stereo top view of the APC. A gallery of different APC views is shown in Figure 4. The dimensions of the complex are 140 Å × 140 Å × 135 Å. The structure of the APC consists of an outer protein wall that encloses a large central cavity which has a diameter of approximately 100 Å and is about 80 Å deep. This cavity has one wide opening located at the top and several smaller openings in the wall and the bottom part of the complex (Figures 3, 4A, 4E, 4G, and 4I). The cavity is partially divided by a rod-like structure that extends from the bottom of the cavity beyond the wall of the particle, forming a prominent protrusion that we call the head (Figures 3A and 4A–4C). The head shields parts of the large opening at the top, like a roof (Figures 4C and 4F). A bridge-like structure connects the head with the outer protein wall (Figures 4A and 4G). In general, the 3D model of the APC is complex and does not reveal any apparent symmetries. This asymmetry, the variable appearance of the complex in different orientations, and the presence of a central cavity are all consistent with the data obtained by negative-staining electron microscopy (Figure 2).

Discussion

Since its discovery in 1995, numerous subunits, regulators, and substrates of the APC have been identified. However, so far no information has been available about the structure and the mechanism of the APC. To address these issues, we have, as a first step, analyzed the structure of the human APC by negative staining and cryo-electron microscopy and have derived a 3D model with a resolution of 24 Å.

Does the APC Use a Cage Mechanism to Ubiquitinate Substrates?

The most remarkable feature revealed by the 3D model of the APC is the presence of a large cavity that is formed by a surrounding protein wall. Although the function of this cavity is unknown, it is tempting to speculate that it may represent a reaction chamber inside of which

ubiquitination reactions take place. Analogous cage mechanisms have been described for other macromolecular machines, in particular for the 26S proteasome and chaperone complexes. The 26S proteasome uses a cylindrical arrangement of subunits to generate reaction chambers in which the proteolytically active sites are shielded from the outside nucleo-cytoplasmic space (Loewe et al., 1995, Groll et al., 1997). Access to this proteolytic compartment is regulated by specialized cap or regulatory complexes that bind to the open ends of the cylindrical protease complex (Peters et al., 1993, Glickman et al., 1998; Braun et al., 1999). Chaperone complexes such as GroEL and TRiC are known to form large cavities whose hydrophobic interior facilitates the folding of polypeptide chains that are captured within these cavities (reviewed by Martin and Hartl, 1997, Bukau and Horwich, 1998; Leroux and Hartl, 2000; for a general discussion of protein machines see Alberts, 1998).

The size of the inner APC cavity would be spaceous enough to harbor ubiquitin-charged ubiquitin-conjugating enzymes and known APC substrates, or at least parts of them, and would therefore be consistent with the possibility that the APC uses a cage mechanism for ubiquitination reactions (see Figure 3A). This hypothesis would predict that at least some of the 11 known APC subunits have a structural role by forming parts of the protein wall that shields the inner cavity from the outside nucleo-cytoplasmic space, whereas other subunits may regulate the access of substrates to catalytically important subunits such as APC11. This notion would help to explain why the APC is composed of so many subunits, even though the subunit APC11 alone is sufficient to mediate ubiquitination reactions in vitro (Gmachl et al., 2000; Leverson et al., 2000). To test this hypothesis, it will in the future be important to localize individual subunits via antibody-labeling techniques. Determining the position of individual subunits within the complex may also provide a framework for assembling the crystal structures of individual APC subunits once these become available.

Will the Structural Features of the APC Apply to Other Cullin and RING Finger–Containing Ubiquitin-Protein Ligases?

The APC, SCF, and VHL complexes contain RING finger and cullin subunits that are essential for their activities, suggesting that these three complexes must have at least some structural features in common. It is unclear, however, if the overall structures of SCF and VHL complexes will turn out to be similar to the 3D structure of the APC because only five subunits of SCF and VHL complexes are known. This difference in subunit complexity could reflect important mechanistic or regulatory differences between the APC and the SCF and VHL complexes. SCF-dependent reactions are controlled at the level of substrates, which are only ubiquitinated by the SCF once they have been phosphorylated at specific sites (reviewed by Deshaies, 1999). In contrast, APC-mediated reactions are only known to be regulated at the level of the APC, whose activity is determined by temporarily controlled associations with CDC20 and CDH1 (reviewed by Zachariae and Nasmyth, 1999). It is, therefore, conceivable that the APC contains more subunits than SCF complexes to allow the regulation of ubiquitination reactions at the level of the ubiquitin-protein ligase. For example, based on the cage hypothesis discussed above it is conceivable that the activity of the APC is regulated by spatially controlling the access of substrates to catalytically important subunits within the APC. In light of this speculation, it will be interesting to determine if the binding of CDC20 or CDH1 to the APC will induce conformational changes that are detectable by cryo-electron microscopical analyses.

Experimental Procedures

Purification of Human APC

Extracts from logarithmically proliferating HeLa cells were prepared in buffer A (20 mM Tris-HCl [pH 7.5], 100 mM NaCl, 0.2% NP-40, 20 mM β-glycerophosphate, 10% glycerol, 1 mM NaF, 0.5 mM DTT) using a Potter-Elvejem glass–Teflon homogenizer. Antibodies raised against a carboxy-terminal 17-mer peptide of human CDC27 were bound to protein A beads at 1 mg antibody per ml beads and incubated with HeLa cell extract for 90 min at 4°C. Beads were washed with buffer A containing 500 mM NaCl, and bound APC was eluted with buffer A plus 1 mg/ml CDC27 peptide for 4 hr or overnight at 4°C. APC fractions were concentrated via ultrafiltration or via vacuum dialysis using collodium membranes (Satorius, Goettingen, Germany). In some experiments, APC and peptide were separated on a Superdex 200 pg column equilibrated with TBS-T (20 mM Tris-HCl, 150 mM NaCl, 0.02% Tween 20, 0.5 mM DTT [pH 7.7]).

Protein Separation Techniques

For analytical gel filtration, a TSK-Gel-G5000PW×l column (Toso Hass, Stuttgart, Germany) equilibrated in TBS-T was used. Ferritin, thyroglobulin, and α2 macroglobolin were used for calibration. For density gradient centrifugation, 10%–30% sucrose gradients were loaded with peptide-eluted APC and centrifuged for 18 hr at 36,000 rpm in an SW40 rotor at 4°C. For the S value determination, bovine serum albumin (4.6S), catalase (11.3S), and thyroglobulin (19.3S) were fractionated and analyzed on a separate gradient. Column and gradient fractions were analyzed by SDS–PAGE followed by silver staining or immunoblotting. For native electrophoresis, proteins were separated as described (Holzl et al., 2000) and detected by silver staining or immunoblotting with specific APC2 antibodies (Gieffers et al., 1999). Bound primary antibodies were detected by a secondary peroxidase-conjugated antibody using enhanced chemiluminescence.

Ubiquitination Assays

Ubiquitination reactions were carried out in a total volume of 10 μl containing 0.5 μg E1, 0.5 μg UBC4, 20 μg ubiquitin, and either 5 μl of peptide-eluted APC, 5 μl of the APC peak fraction after the gel filtration, or 2.5 μl of the concentrated peak fraction, respectively. As substrate, we used an iodinated N-terminal recombinant fragment of sea urchin cyclin B (amino acids 13–110) (Holloway et al., 1993). Samples were taken after 0, 10, and 20 min, and the reactions were stopped by addition of SDS sample buffer and analyzed by SDS–PAGE and phosphoimaging.

Negative-Stain Electron Microscopy

Five microliters of purified APC was applied to 400 mesh copper grids, coated with a thin carbon support film, and glow-discharge treated for 20 s before use (Harris, 1997). The adsorbed APC was washed four times with 20 μl droplets of distilled water and negatively stained with 2% (w/v) aqueous ammonium molybdate adjusted to pH 7.0 with NaOH. Microscopy was performed using a Zeiss EM900 transmission electron microscope, routinely at 50,000× magnification.

Cryo-Electron Microscopy and Image Processing

Cryo-electron microscopy was performed using a Philips C20 electron microscope equipped with a field emission electron source

operating at 160 kV accelerating voltage. Images were recorded under low-dose conditions using a Kodak SO163 film at 50,000× instrumental magnification at 1.5 μm underfocus. Electron micrographs were digitized on a drum scanner with a scan step of 2400 dpi, which provided a sampling step of 2.1 Å at the specimen level. Image processing was performed as described (Dube et al., 1998).

Acknowledgments

We are greatful to Karl Mechtler and Ika Gorny for peptide syntheses, Karin Paiha and Peter Steinlein for technical help with the images, and Kim Nasmyth for comments on the manuscript. TEM facilities (J .R. H.) were made available by Prof. Albrecht Fischer (Institute of Zoology, Mainz). Research in the laboratory of J.-M. P. was supported by Boehringer Ingelheim and by grants from the Austrian Science Fund (FWF P13865-BIO) and the Austrian Industrial Research Promotion Fund (FFF 802569).

Received December 18, 2000; revised February 26, 2001.

References

Alberts, B. (1998). The cell as a collection of protein machines: preparing the next generation of molecular biologists. Cell *92*, 291–294.

Baumeister, W., Walz, J., Zuhl, F., and Seemuller, E. (1998). The proteasome: paradigm of a self-compartmentalizing protease. Cell *92*, 367–380.

Braun, B.C., Glickman, M., Kraft, R., Dahlmann, B., Kloetzel, P.M., Finley, D., and Schmidt, M. (1999). The base of the proteasome regulatory particle exhibits chaperone-like activity. Nat. Cell Biol. *1*, 221–226.

Bukau, B., and Horwich, A.L. (1998). The Hsp70 and Hsp60 chaperone machines. Cell *92*, 351–366.

Deshaies, R.J. (1999). SCF and Cullin/Ring H2-based ubiquitin ligases. Annu. Rev. Cell Dev. Biol. *15*, 435–467.

Dube, P., Bacher, G., Stark, H., Mueller, F., Zemlin, F., van Heel, M., and Brimacombe, R. (1998). Correlation of the expansion segments in mammalian rRNA with the fine structure of the 80 S ribosome; a cryoelectron microscopic reconstruction of the rabbit reticulocyte ribosome at 21 Å resolution. J. Mol. Biol. *279*, 403–421.

Gieffers, C., Peters, B.H., Kramer, E.R., Dotti, C.G., and Peters, J.M. (1999). Expression of the CDH1-associated form of the anaphase-promoting complex in postmitotic neurons. Proc. Natl. Acad. Sci. USA *96*, 11317–11322.

Glickman, M.H., Rubin, D.M., Coux, O., Wefes, I., Pfeifer, G., Cjeka, Z., Baumeister, W., Fried, V.A., and Finley, D. (1998). A subcomplex of the proteasome regulatory particle required for ubiquitin-conjugate degradation and related to the COP9-signalosome and eIF3. Cell *94*, 615–623.

Gmachl, M., Gieffers, C., Podtelejnikov, A.V., Mann, M., and Peters, J.M. (2000). The RING-H2 finger protein APC11 and the E2 enzyme UBC4 are sufficient to ubiquitinate substrates of the anaphase-promoting complex. Proc. Natl. Acad. Sci. USA *97*, 8973–8978.

Groll, M., Ditzel, L., Lowe, J., Stock, D., Bochtler, M., Bartunik, H.D., and Huber, R. (1997). Structure of 20S proteasome from yeast at 2.4 Å resolution. Nature *386*, 463–471.

Grossberger, R., Gieffers, C., Zachariae, W., Podtelejnikov, A.V., Schleiffer, A., Nasmyth, K., Mann, M., and Peters, J.M. (1999). Characterization of the DOC1/APC10 subunit of the yeast and the human anaphase-promoting complex. J. Biol. Chem. *274*, 14500–14507.

Harris, J.R. (1997). Negative Staining and Cryoelectron Microscopy: The Thin Film Techniques (Oxford, UK: BIOS Scientific Ltd.).

Holloway, S.L., Glotzer, M., King, R.W., and Murray, A.W. (1993). Anaphase is initiated by proteolysis rather than by the inactivation of maturation-promoting factor. Cell *73*, 1393–1402.

Holzl, H., Kapelari, B., Kellermann, J., Seemuller, E., Sumegi, M., Udvardy, A., Medalia, O., Sperling, J., Muller, S.A., Engel, A., and Baumeister, W. (2000). The regulatory complex of Drosophila melanogaster 26S proteasomes. Subunit composition and localization of a deubiquitylating enzyme. J. Cell Biol. *150*, 119–130.

Huang, L., Kinnucan, E., Wang, G., Beaudenon, S., Howley, P.M., Huibregtse, J.M., and Pavletich, N.P. (1999). Structure of an E6AP-UbcH7 complex: insights into ubiquitination by the E2–E3 enzyme cascade. Science *286*, 1321–1326.

Irniger, S., Piatti, S., Michaelis, C., and Nasmyth, K. (1995). Genes involved in sister chromatid separation are needed for B-type cyclin proteolysis in budding yeast. Cell *81*, 269–278.

Jiang, F., and Basavappa, R. (1999). Crystal structure of the cyclin-specific ubiquitin-conjugating enzyme from clam, E2-C, at 2.0 Å resolution. Biochemistry *38*, 6471–6478.

Joazeiro, C.A., and Weissman, A.M. (2000). RING finger proteins: mediators of ubiquitin ligase activity. Cell *102*, 549–552.

King, R.W., Peters, J.M., Tugendreich, S., Rolfe, M., Hieter, P., and Kirschner, M.W. (1995). A 20S complex containing CDC27 and CDC16 catalyzes the mitosis-specific conjugation of ubiquitin to cyclin B. Cell *81*, 279–288.

Kussie, P.H., Gorina, S., Marechal, V., Elenbaas, B., Moreau, J., Levine, A.J., and Pavletich, N.P. (1996). Structure of the MDM2 oncoprotein bound to the p53 tumor suppressor transactivation domain. Science *274*, 948–953.

Leroux, M.R., and Hartl, F.U. (2000). Protein folding: versatility of the cytosolic chaperonin TRiC/CCT. Curr. Biol. *10*, R260–264.

Leverson, J.D., Joazeiro, C.A., Page, A.M., Huang, H., Hieter, P., and Hunter, T. (2000). The APC11 RING-H2 finger mediates E2-dependent ubiquitination. Mol. Biol. Cell *11*, 2315–2325.

Loewe, J., Stock, D., Jap, B., Zwickl, P., Baumeister, W., and Huber, R. (1995). Crystal structure of the 20S proteasome from the archaeon T. acidophilum at 3.4 Å resolution. Science *268*, 533–539.

Martin, J., and Hartl, F.U. (1997). Chaperone-assisted protein folding. Curr. Opin. Struct. Biol. *7*, 41–52.

Morgan, D.O. (1999). Regulation of the APC and the exit from mitosis. Nat. Cell Biol. *1*, E47–E53.

Nasmyth, K., Peters, J.M., and Uhlmann, F. (2000). Splitting the chromosome: cutting the ties that bind sister chromatids. Science *288*, 1379–1385.

Peters, J.-M. (1994). Proteasomes: protein degradation machines of the cell. Trends Biochem. Sci. *19*, 377–382.

Peters, J.-M. (1999). Subunits and substrates of the anaphase-promoting complex. Exp. Cell Res. *248*, 339–349.

Peters, J.-M., Cejka, Z., Harris, J.R., Kleinschmidt, J.A., and Baumeister, W. (1993). Structural features of the 26 S proteasome complex. J. Mol. Biol. *234*, 932–937.

Scheffner, M., Nuber, U., and Huibregtse, J.M. (1995). Protein ubiquitination involving an E1–E2-E3 enzyme ubiquitin thioester cascade. Nature *373*, 81–83.

Schulman, B.A., Carrano, A.C., Jeffrey, P.D., Bowen, Z., Kinnucan, E.R., Finnin, M.S., Elledge, S.J., Harper, J.W., Pagano, M., and Pavletich, N.P. (2000). Insights into SCF ubiquitin ligases from the structure of the Skp1-Skp2 complex. Nature *408*, 381–386.

Stebbins, C.E., Kaelin, W.G., Jr., and Pavletich, N.P. (1999). Structure of the VHL-ElonginC-ElonginB complex: implications for VHL tumor suppressor function. Science *284*, 455–461.

Sudakin, V., Ganoth, D., Dahan, A., Heller, H., Hershko, J., Luca, F.C., Ruderman, J.V., and Hershko, A. (1995). The cyclosome, a large complex containing cyclin-selective ubiquitin ligase activity, targets cyclins for destruction at the end of mitosis. Mol. Biol. Cell *6*, 185–197.

Tyers, M., and Willems, A.R. (1999). One ring to rule a superfamily of E3 ubiquitin ligases. Science *284*, 603–604.

Varshavsky, A. (1997). The ubiquitin system. Trends Biochem. Sci. *22*, 383–387.

Vijay-Kumar, S., Bugg, C.E., Wilkinson, K.D., Vierstra, R.D., Hatfield, P.M., and Cook, W.J. (1987). Comparison of the three-dimensional structures of human, yeast, and oat ubiquitin. J. Biol. Chem. *262*, 6396–6399.

Yu, H., Peters, J.M., King, R.W., Page, A.M., Hieter, P., and Kirschner,

M.W. (1998). Identification of a cullin homology region in a subunit of the anaphase-promoting complex. Science *279*, 1219–1222.

Zachariae, W., and Nasmyth, K. (1999). Whose end is destruction: cell division and the anaphase-promoting complex. Genes Dev. *13*, 2039–2058.

Zachariae, W., Shevchenko, A., Andrews, P.D., Ciosk, R., Galova, M., Stark, M.J.R., Mann, M., and Nasmyth, K. (1998). Mass spectrometric analysis of the anaphase promoting complex from yeast: identification of a subunit related to Cullins. Science *279*, 1216–1219.

Zheng, N., Wang, P., Jeffrey, P.D., and Pavletich, N.P. (2000). Structure of a c-Cbl-UbcH7 complex: RING domain function in ubiquitin-protein ligases. Cell *102*, 533–539.